EUROPEAN ORGANIZATION FOR NUCLEAR RESEARCH

CERN-EP/84-85
18 July 1984

$p\bar{p}$ ANNIHILATIONS AT REST IN HYDROGEN GAS: REPORT ON PRELIMINARY RESULTS OF THE ASTERIX EXPERIMENT AT LEAR

The ASTERIX*) Collaboration

CERN[1], Mainz[2], München[3], Orsay (LAL)[4], TRIUMF-Vancouver-Victoria[5], Zurich[6]

S. Ahmad[4], C. Amsler[6], R. Armenteros[4], E.G. Auld[5], D. Axen[5], D. Bailey[1], S. Barlag[1], G. Beer[5], J.C. Bizot[4], M. Caria[6], M. Comyn[5], W. Dahme[3], B. Delcourt[4], M. Doser[6], K.D. Duch[2], K. Erdmann[5], F. Feld[3], U. Gastaldi[1], M. Heel[2], B. Howard[5], R. Howard[5], J. Jeanjean[4], H. Kalinowsky[2], F. Kayser[2], E. Klempt[2], R. Landua[1], G. Marshall[5], H. Nguyen[4], N. Prevot[4], L. Robertson[5], C. Sabev, U. Schaefer[3], R. Schneider[2], O. Schreiber[2], U. Straumann[2], P. Truoel[6], B.L. White[5], W.R. Wodrich[3], M. Ziegler[2].

(Presented by F. Feld)

Paper given at the
International School of Physics of Exotic Atoms,
4th Course: Fundamental Interactions in Low-Energy Systems,
Erice, 31 March-6 April 1984

---

*) Antiproton STop Experiment with tRigger on Initial X-rays.

$p\bar{p}$ ANNIHILATIONS AT REST IN HYDROGEN GAS:

REPORT ON PRELIMINARY RESULTS OF THE ASTERIX EXPERIMENT AT LEAR

The ASTERIX* Collaboration

S. Ahmad[4], C. Amsler[6], R. Armenteros[4], E.G. Auld[5], D. Axen[6], D. Bailey[1], S. Barlag[1], G. Beer[5], J.C. Bizot[4], M. Caria[2], M. Comyn[5], W. Dahme[3], B. Delcourt[4], M. Doser[6], K.D. Duch[2], K. Erdmann[5], F. Feld[3], U. Gastaldi[1], M. Heel[2], B. Howard[5], R. Howard[5], J. Jeanjean[4], H. Kalinowsky[2], F. Kayser[2], E. Klempt[2], R. Landua[1], G. Marshall[1], H. Nguyen[4], N. Prevot[4], L. Robertson[5], C. Sabev, U. Schaefer[3], R. Schneider[2], O. Schreiber[2], U. Straumann[2], P. Truoel[6], B.L. White[5], W.R. Wodrich[3], M. Ziegler[2]

(Presented by F. Feld)

INTRODUCTION AND CONCLUSIONS

The ASTERIX experiment has been set up to study $p\bar{p}$-annihilations at rest into $q\bar{q}$-mesons and other boson resonances like glueballs (gg, ggg), hybrids ($q\bar{q}g$), baryonia ($qq\bar{q}\bar{q}$) and $N\bar{N}$ bound states from S and P states of the $p\bar{p}$ atom. A detailed description of the apparatus can be found in the proposal[1)] and in the contributions to the LEAR Erice Workshop 1982[2,3)]

The installation of the experiment started in 1982; the first antiprotons for tests arrived in July 1983 and during December 1983 we had our first production runs with an antiproton beam of 308 MeV/c before moderation. In about 50 spills of 1 hour we recorded a total of about 4×10^6 events on tape. For part of the data the trigger required an antiproton stopping in the target, while for the remainder in additon an X-ray candidate was requested. During January 1984 the events were reconstructed and

---

*) Antiproton STop Experiment with tRigger on Initial X-rays.
CERN[1], Mainz[2], Munich[3], Orsay[4] (LAL), TRIUMF-Vancouver-Victoria[5], Zurich[6]

about 8×10^5 events were found to have a reconstructed annihilation vertex inside the Hydrogen target. The analysis of these data, which is still in progress, has so far led to the following preliminary results:

The 2P level of the $p\bar{p}$ atom is reached in the atomic cascade in H_2 gas at NTP with a probability of about 10% with emission of an X-ray of the L series (L_α = 1.7 keV, L_β = 2.4 keV, L_∞ = 3.1 keV)

In fully reconstructed annihilation channels involving besides charged particles 0 or 1 neutral particle, we observe well known mesons (π, K, η, ρ, ω, f, A_2) at their nominal masses.

When comparing relative branching ratios (e.g. $p\bar{p} \to \rho^0\pi^0 / p\bar{p} \to f^0\pi^0$) obtained in bubble chamber experiments[4] (assumed to be S-wave annihilation, because of strong Stark mixing in higher atomic levels leading to annihilation from nS levels) with our data once requiring a stopped $\bar{p}$ only (mixture of S- and P-wave annihilation) and secondly asking also for the L X-ray to be detected in coincidence (P-wave annihilation), we find a continuous change. Preliminary we conclude that one has $\sim$ 10-40% S-wave and $\sim$ 60-90% P-wave annihilation in atmospheric H_2 gas.

In the following sections we recall briefly the main features of the experiment and then present some of our observations. We stress the preliminary nature of the spectra that we show.

For the purpose of this report all observed charged tracks are called Pions. No corrections have been made for the small fraction of Kaon and electron (Dalitz-pairs) tracks contained in the spectra.

EXPERIMENTAL SET-UP

A schematic view of the detector is shown in Fig. 1. Antiprotons enter a solenoidal magnet along its axis and are brought to rest in a cylindrical hydrogen gas target. This target is surrounded by a cylindrical projection chamber (XDC for X-ray Drift Chamber) which measures energy and conversion point of the X-rays emitted during the de-excitation of the $p\bar{p}$ atom. This chamber also gives the initial track element for charged particles emerging from the annihilation. The continuation of these tracks is identified by seven cylindrical multi-wire proportional chambers (C1, C2, Q1, Q2, P1, Q3, P2). Gammas produced in the annihilation are partially converted in lead sheets (0.9 radiation length) placed at the two endcaps and immediately in front of the chamber Q3. The hexagonal lead sheets at the endcaps are preceeded by a MWPC to veto against charged particles and followed by two MWPC's to identify the electromagnetic shower. From the gamma conversion point, determined in this way, and the annihilation vertex reconstructed

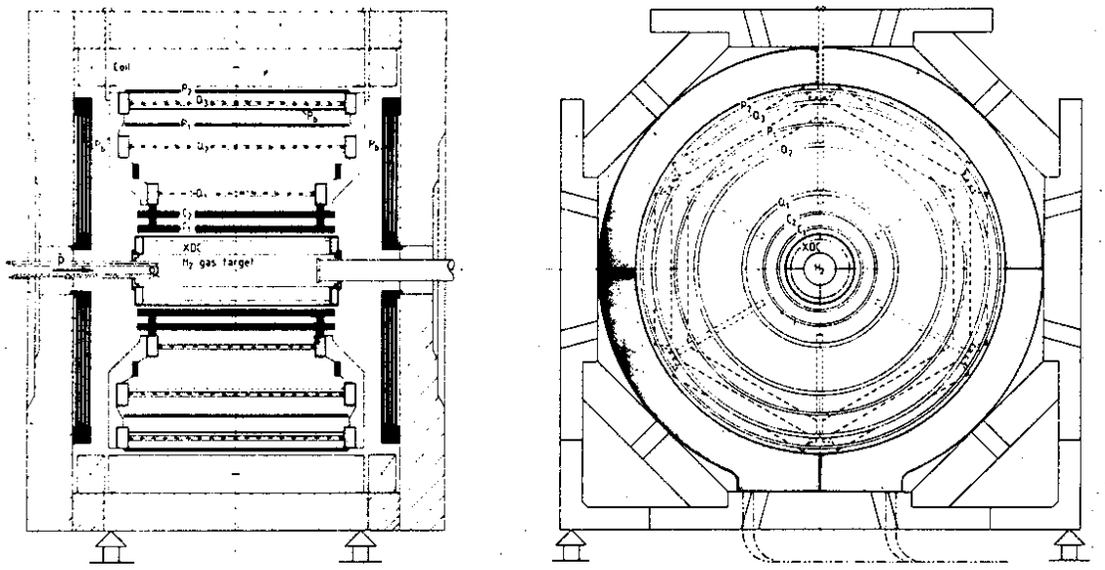

Fig. 1. Schematic side and front view of the ASTERIX detector: XDC: X-ray Drift Chamber (three-dimensional projection chamber); C1, C2, Q1, Q2, Q3 and endcaps: multiwire proportional chambers with anode and cathode strip readout; P1, P2: multiwire proportional chambers with anode readout

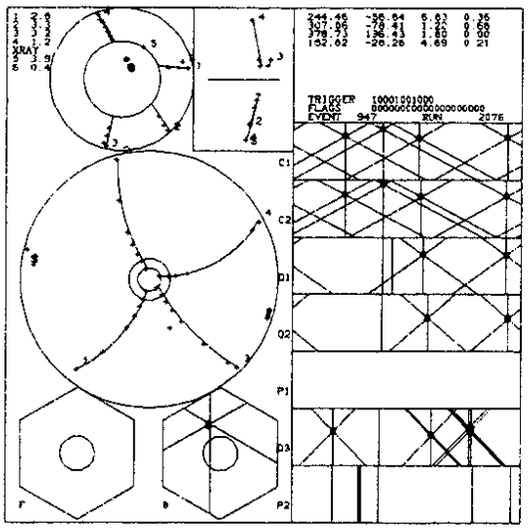

Fig. 2. Reconstructed event:
top left: magnified view of the charge observed in the XDC. Four tracks and an X-ray converted near the mylar foil are clearly visible; centre left: the four tracks reconstructed using the hit wires pattern of the cyl. MWPC's (right) and a reconstructed γ conversion point (indicated by $); a second γ has converted in the backward endcap detector (bottom left).

from the tracks of the charged annihilation products, we obtain the direction of flight of the gammas. For illustration we show an event as seen by the computer in Fig. 2. The distribution of reconstructed vertices for all events of one run is displayed in Fig. 3. Antiprotons stopped in the H_2 gas volume are clearly distinguished from those stopping in the entrance and exit scintillators as well as in the XDC counter gas (argon) and the Mylar foil separating hydrogen and argon. The energy of the X-rays is determined with a resolution of $\pm$ 11% at 5.5 KeV, and the momenta of the charged particles are measured with a resoluton of $\pm$ 4% at 500 MeV/c.

PRELIMINARY RESULTS

Protonium Spectroscopy

Figure 4a shows the X-ray spectrum obtained during $\bar{p}_{STOP}$ trigger runs. The strong signal in the energy region between 1 and 4 keV corresponds to L transitions populating the atomic 2P level. The L_α line at 1.7 keV is clarly distinguished from the L_β.... L_∞ lines. The radial distribution of the associated absorption points (Fig. 4b) confirms that these X-rays are produced inside the H_2 target.

The fact that the spectrum contains almost exclusively L-line events reconfirms the earlier observation by E. Auld et al.[5] that the 2P level (which has a radiative width of 10^{-11} sec and therefore does not live long enough to mix with the 2S level by collisional Stark mixing in 1 atm gas) decays dominantly via annihilation.

The events below the L_α line are most likely M X-rays emitted from high levels that are still able to traverse the 6μ Mylar foil separating the counter gas from the target gas.

X-rays emitted from transitions to the atomic 1S level (K-lines) are expected at energies of about 9 keV. Only few events are observed in this energy region. It should be mentioned that the X-ray detector was operated initially at a high gas gain to ensure a proper identification of the L-transitions to study annihilations from the atomic 2P level. This operating condition led to a deteriorated energy scale for energies larger than 6 keV. In subsequent runs the gas gain was lowered, but the analysis of this data is still in progress. However, a weak population of the atomic 1S-level can already be concluded from the scarcity of events observed above 6 keV.

In Fig. 4a we also compare the events with an associated reconstructed vertex in H_2 with those events where the vertex was found in the argon gas of the XDC. For these events the 3 KeV

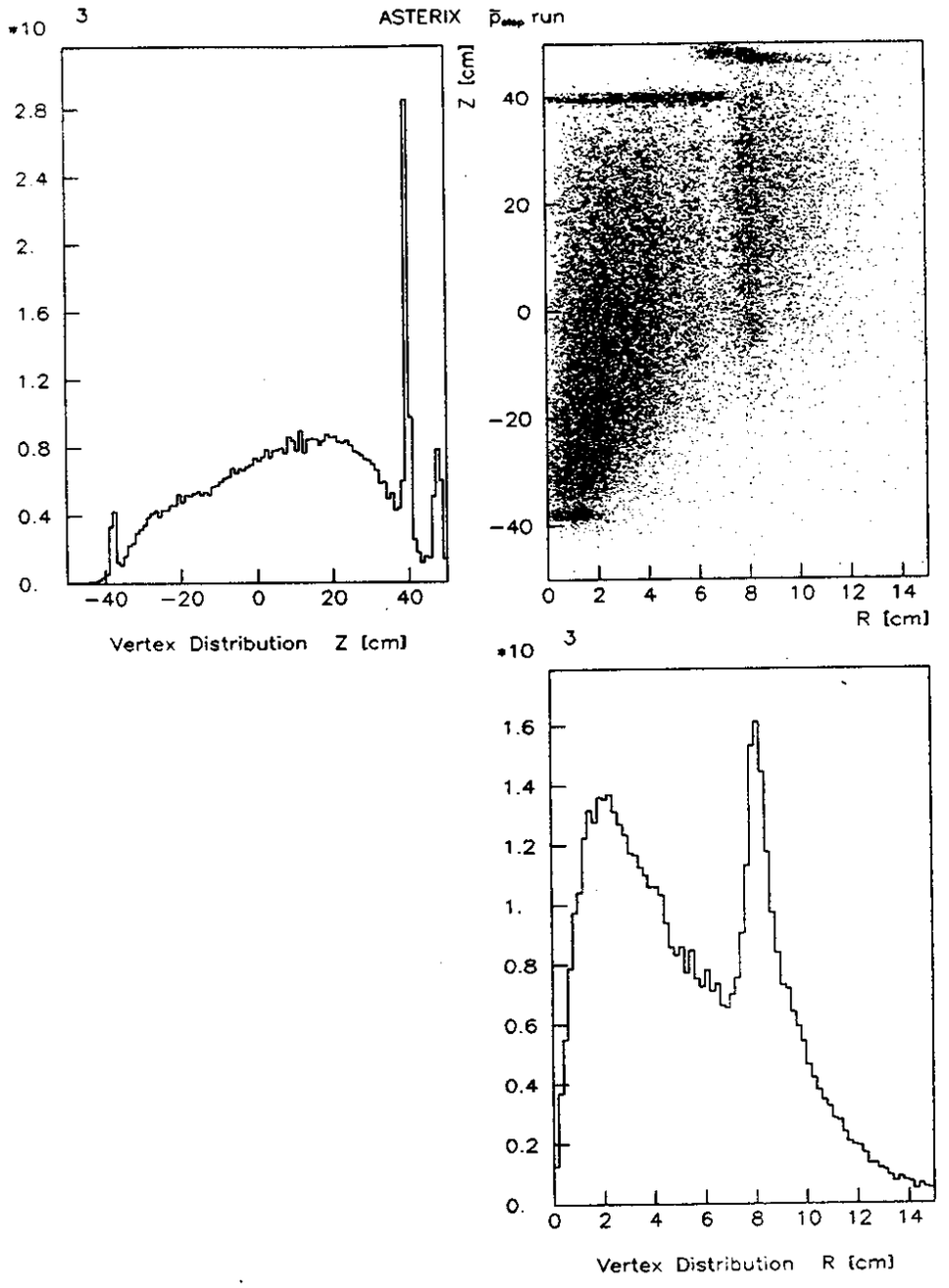

Fig. 3. Distribution of reconstructed annihilation vertices for one run. The three sharp peaks in the z-distribution (top left) represent annihilations occurring in the entrance (T2) and exit (T4) scintillators and the aluminium frame of the XDC, respectively. Annihilations in the thin (6μ) Mylar foil separating the H_2 target from the XCD counter gas lead to the sharp peak in the r-distribution.

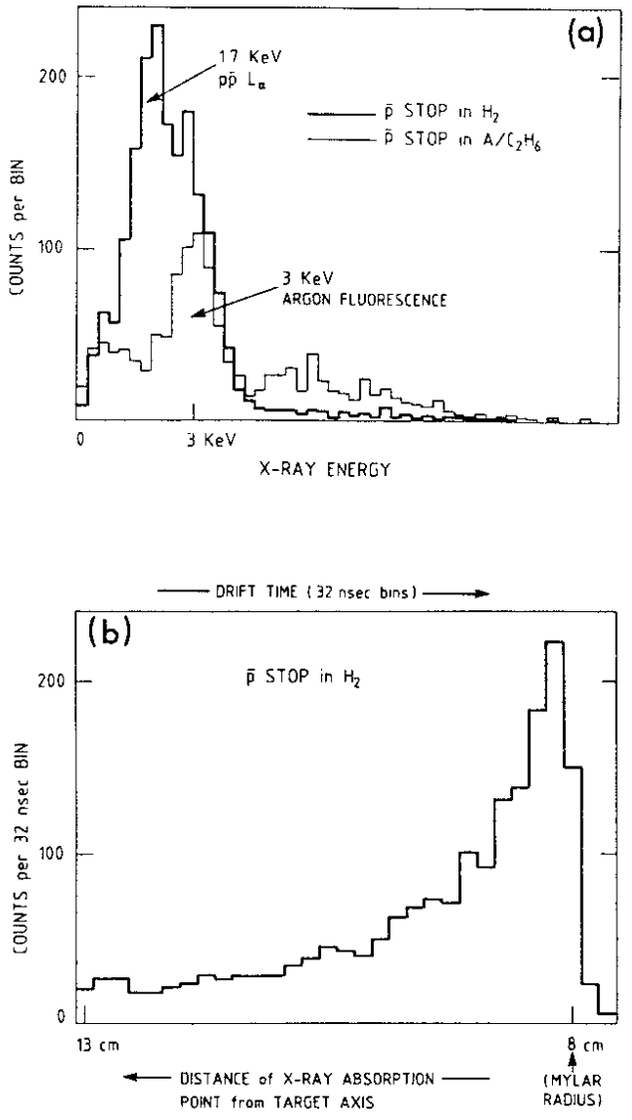

Fig. 4. X-ray energy spectrum (a) and distribution of associated absorption points (b) for $p\bar{p}$ annihilations with identified annihilation vertex inside a fiducial volume in the H_2 gas target. Nearly background free, the spectrum is dominated by the transitions feeding the atomic 2P-level. For comparison the spectrum obtained for events with identified vertex inside the XDC counter gas volume is shown. The 3 keV argon fluorescence line serves for on-line energy monitoring.

argon fluorescence line due to scattered antiprotons is apparent. This line serves as an online in beam energy calibration monitor.

Two Collinear Tracks

In Fig. 5 we show the momentum spectrum for events with two collinear tracks of total charge 0. Two peaks expected for $p\bar{p} \to \pi^+\pi^-$ and $p\bar{p} \to K^+K^-$ events are well separated. We find for the ratio $p\bar{p} \to K^+K^-$ to $p\bar{p} \to \pi^+\pi^-$ $\sim 15\%$ compared to $\sim 30\%$ found in bubble chamber experiments[4].

The $\pi^+\pi^-$ X-channel

Figure 6 displays a scatterplot (including projections) of the missing energy and the missing mass squared recoiling against two particles of opposite charge. The peaks in the missing mass spectrum correspond to the neutrals π^0, η^0, ρ^0/ω^0 respectively. In the scatterplot the energies of the recoiling neutrals are indicated for the case in which $\pi^+\pi^-$ were the decay products of ρ^0 and f^0. The dashed line represents the fraction of events which passed the kinematics fit to the $p\bar{p} \to \pi^+\pi^-\pi^0$ hypothesis. The resulting three-body Dalitz plot (Fig. 7) shows that this reaction is dominated by ρ resonance production. The limited solid angle of our detector imposes a smaller probability for detecting ρ^0 as compared to $\rho^\pm$, thus explaining the apparent smaller fraction of $\rho^0\pi^0$ events. This limit applies only up to invariant masses of the $\pi^+\pi^-$ pair of ~ 1.0 GeV. Above the ρ^0 a strong peak is seen, which was not seen previously in bubble chamber experiments[4], corresponding in width and mass to the f^0. When imposing the presence of an L X-ray, which feeds the atomic 2P state, in coincidence the fraction of $f^0\pi^0$ events increases compared to the number of $\rho^0\pi^0$ events. A detailed fit of the Dalitz plot in view of the different contributing amplitudes is currently in progress.

The $2\pi^+2\pi^-$ X-channel

For the events with four observed tracks of total charge 0 we show the scatterplot of missing mass squared versus missing energy recoiling against the 4 pions (Fig. 8). We observe mainly 4-pion ($2\pi^+2\pi^-$) and 5-pion ($2\pi^+2\pi^-\pi^0$) events. These two channels can be identified nearly background free by kinematical fitting. In this first run we obtained ~ 3500 $p\bar{p} \to 2\pi^+2\pi^-\pi^0$ events for which we show in Fig. 9 the invariant mass combinations of the 3-pion versus the 2-pion subsystems. In the projections the η^0, ω^0 and ρ^0 can be distinguished clearly. The scatterplot also shows a strong bump of $p\bar{p} \to \omega^0\rho^0$ production.

Finally we should like to mention that selecting annihilations with Kaons present in the final state is in progress. We have so far identified about 10^3 $p\bar{p} \to \pi^+\pi^-K^+K^-$ events and a few $p\bar{p} \to K^0\bar{K}^0$ events.

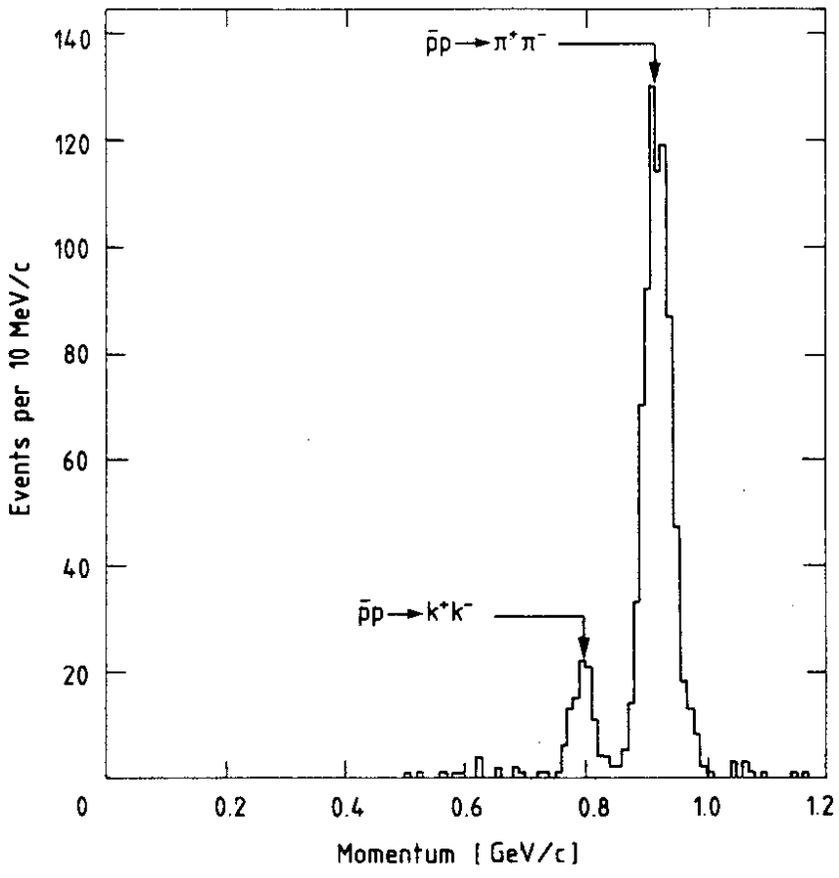

Fig. 5. Momentum spectrum of two collinear particles of opposite charge. Two peaks corresponding to annihilatons into $\pi^+\pi^-$ and K^+K^- respectively, are clearly visible at their expected positions.

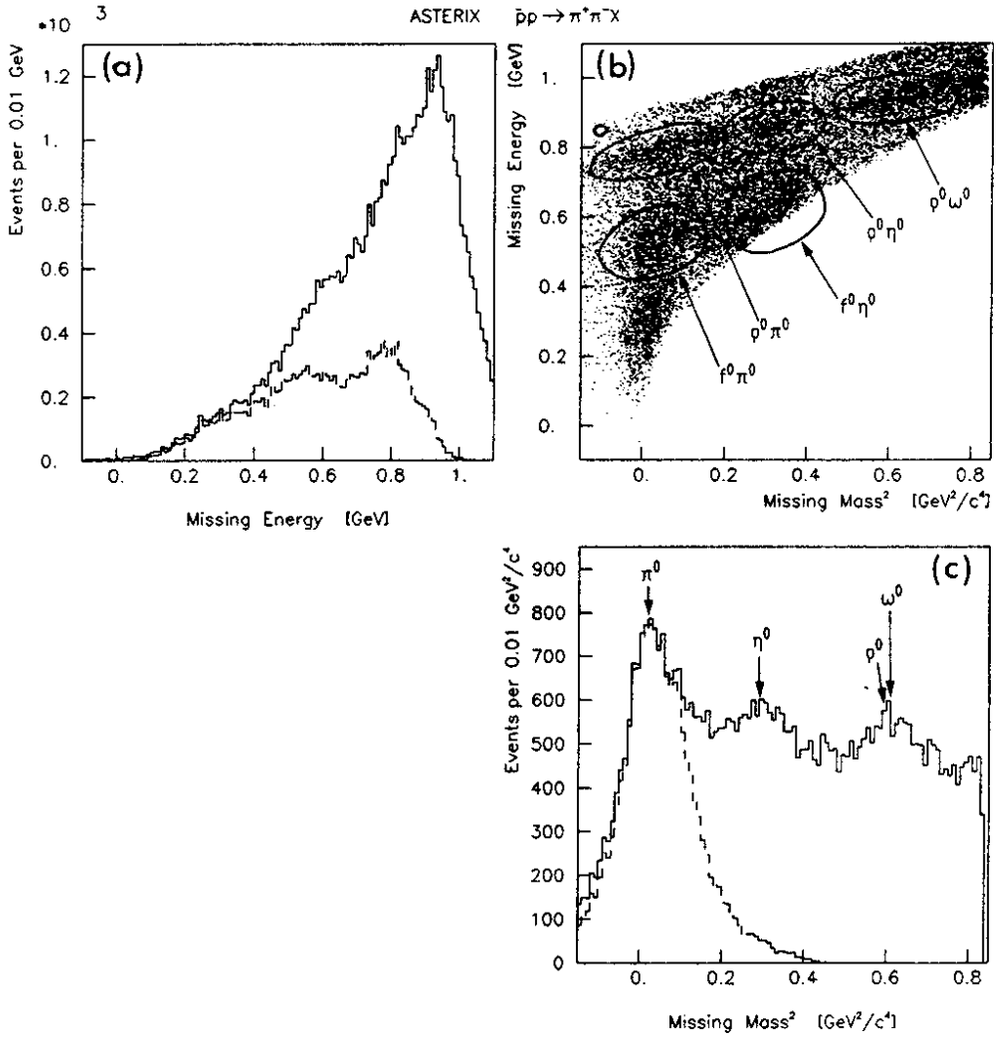

Fig. 6. Scatterplot (b) and projections of the missing mass squared (c) and the missing energy (a) recoiling against two particles of opposite charge. Energies and masses of possible two-body annihilations are indicated. The dashed line shows the fraction of events that passed the kinematics fit to the $p\bar{p} \to \pi^+\pi^-\pi^0$ hypothesis.

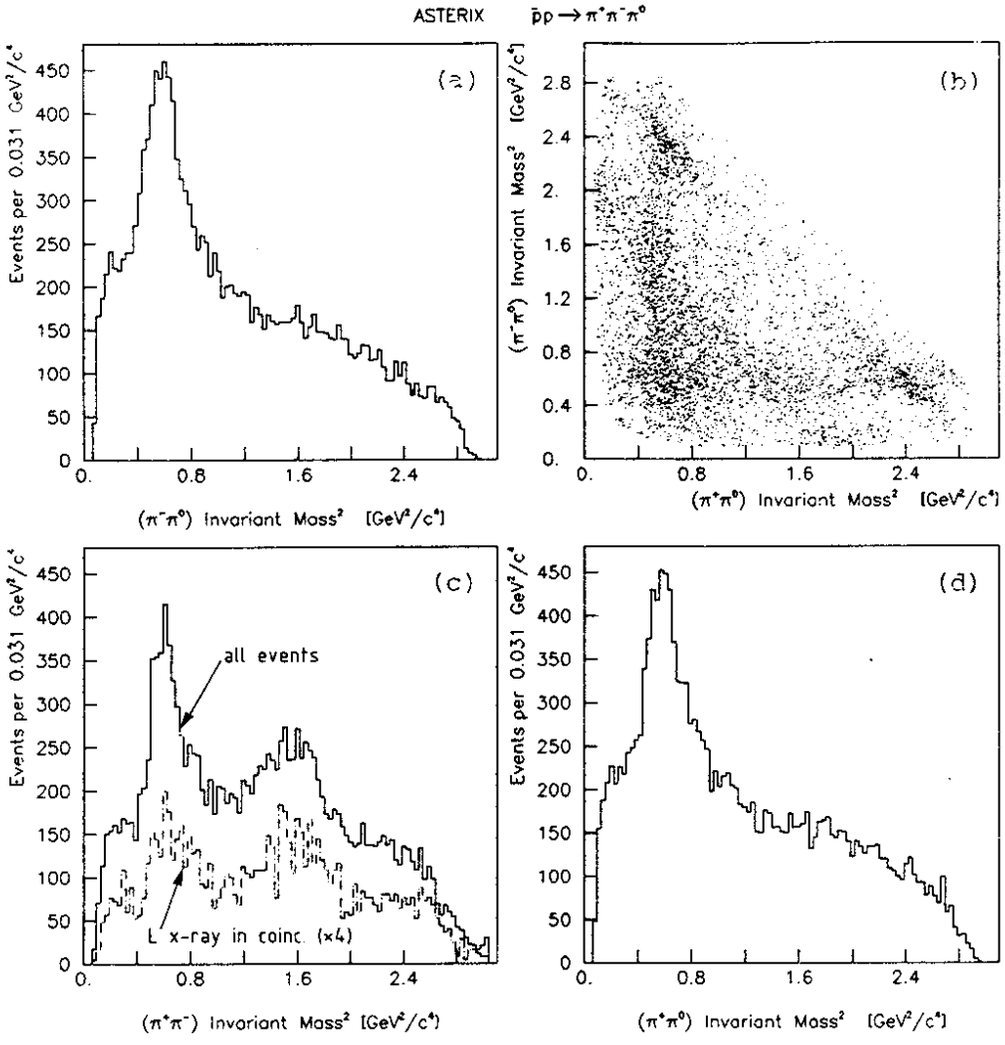

Fig. 7. Dalitz plot and invariant mass squared projections of pion pairs for the events that passed the kinematics fit to the $p\bar{p} \rightarrow \pi^+\pi^-\pi^0$ hypothesis. Large $\rho^{0\pm}$ and f^0 production can be seen. The dashed dotted line in Fig. 7c shows the spectrum obtained with an L X-ray detected in coincidence.

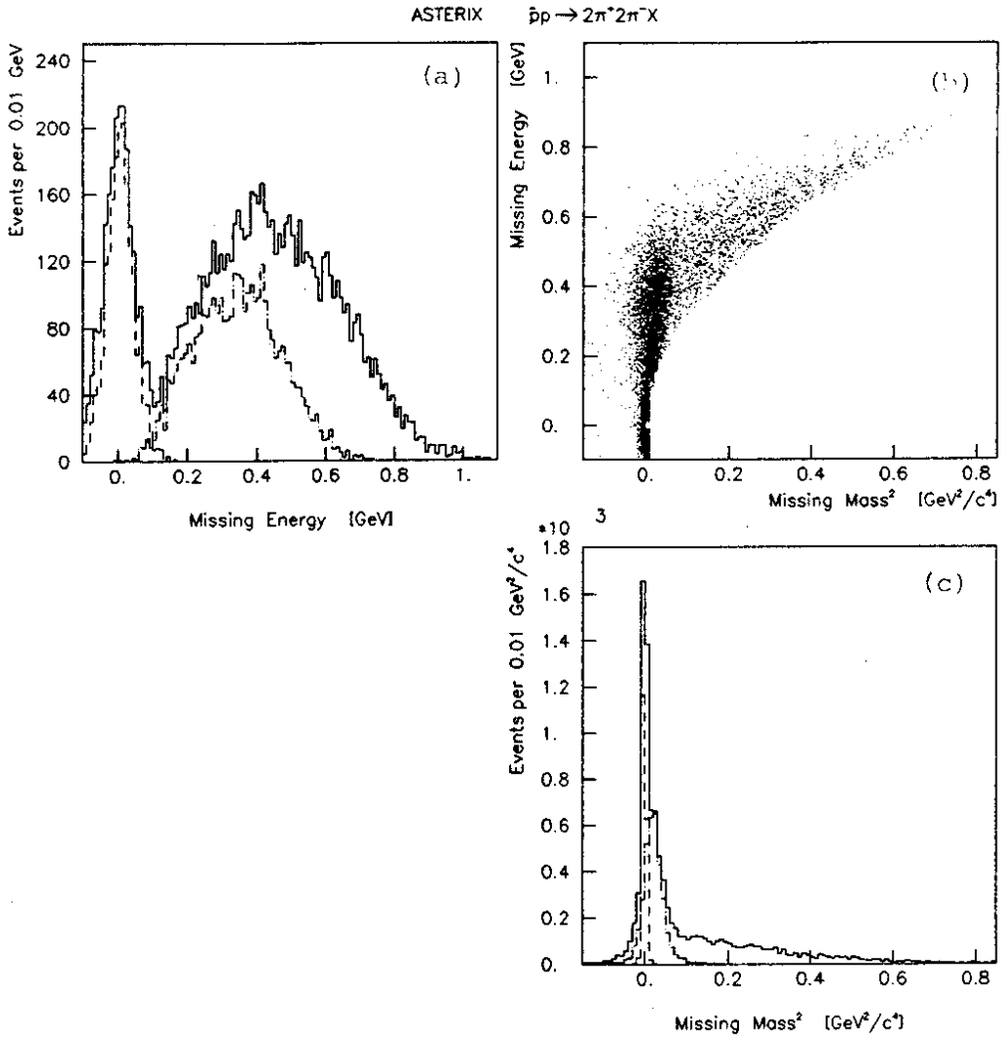

Fig. 8. Scatterplot (b) and projection of the missing mass squared (c) and the missing energy (a) recoiling against two pion pairs of opposite charge. The dashed and dashed-dotted lines indicate the fractions of events that passed the kinematics fit to the $p\bar{p} \rightarrow 2\pi^+2\pi^-$ and the $p\bar{p} \rightarrow 2\pi^+2\pi^-\pi^0$ hypothesis, respectively. Good separation is obtained.

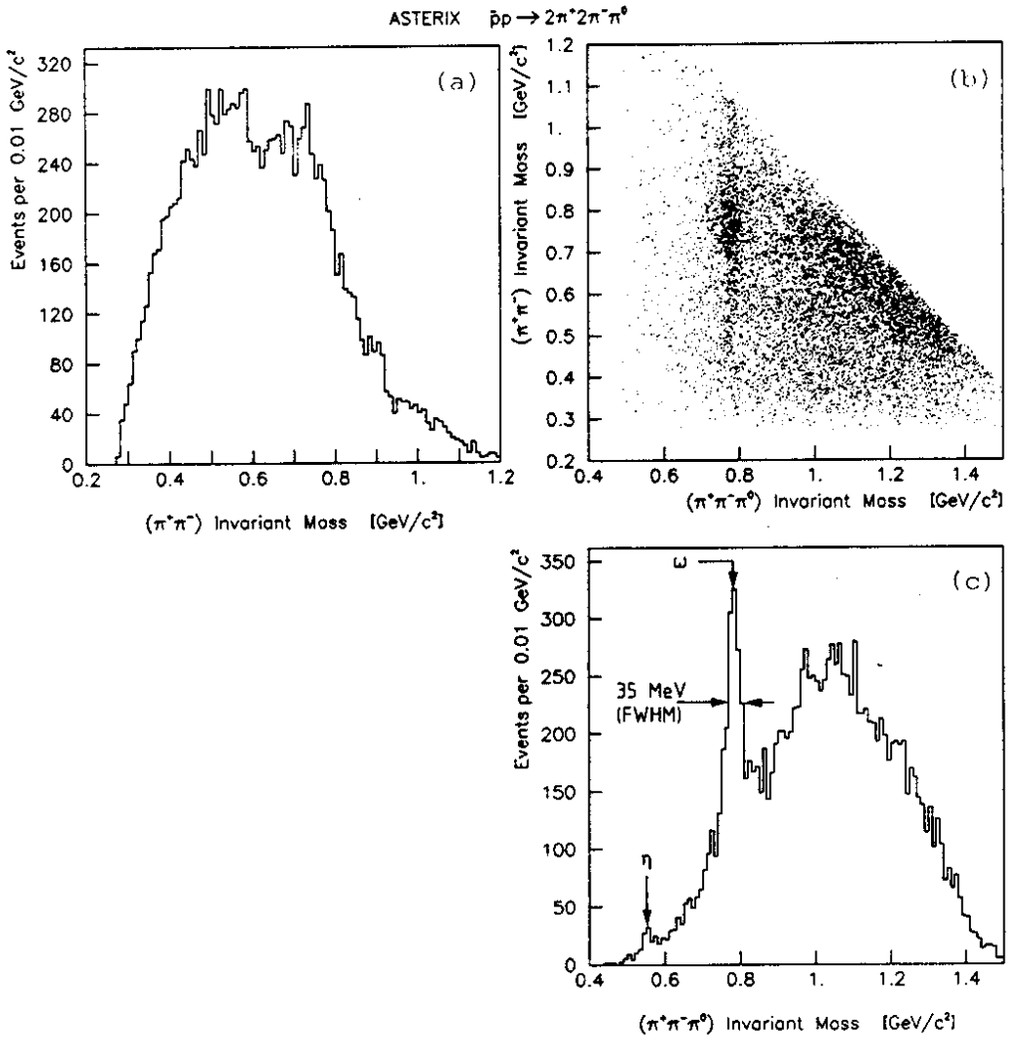

Fig. 9. Scatterplot (incl. projections) of the invariant mass of three pion combinations versus two pion combinations for events which passed the kinematics fit to the $p\bar{p} \rightarrow 2\pi^+\pi^-\pi^0$ hypothesis. Large ω production is observed. The ω recoils predominantly against a ρ.

REFERENCES

1. R. Armenteros et al., A study of $p\bar{p}$ interactions at rest in a H_2 gas target at LEAR, CERN/PSCC 80-101 (1980).

2. S. Ahmad et al., Protonium Spectroscpy and Identification of P-Wave and S-Wave Initial States of $p\bar{p}$-Annihilations at rest with the ASTERIX Experiment at LEAR, in: "Physics at LEAR with Cooled Low Energy antiprotons", U. Gastaldi and R. Klapisch, ed., Plenum Press, New York (1984) 109.

3. S. Ahmad et al., $(q\bar{q})$ Spectroscopy and Search for Glueballs, Baryonia and other Boson Resonances in $p\bar{p}$-Annhilations at Rest with the ASTERIX Experiment at LEAR, in:"Physics at LEAR with Cooled Low Energy antiprotons", U. Gastaldi and R. Klapisch, ed., Plenum Press, New York (1984) 253.

4. R. Armenteros and B. French, $N\bar{N}$ Interactions, in: "High Energy Physics", E.H.S. Burhop, ed., Academic Press Inc., New York (1969).

5. E. Auld et al., Phys. Lett. 77B:454 (1978).